ELSEVIER

Journal of Chromatography A, 945 (2002) 45–63

JOURNAL OF CHROMATOGRAPHY A

www.elsevier.com/locate/chroma

Towards ochratoxin A selective molecularly imprinted polymers for solid-phase extraction ☆

Justus Jodlbauer, Norbert M. Maier*, Wolfgang Lindner*

Institute of Analytical Chemistry, University of Vienna, Währinger Strasse 38, A-1090 Vienna, Austria

Received 11 September 2001; received in revised form 12 November 2001; accepted 12 November 2001

Abstract

Molecularly imprinted polymers (MIPs) displaying selective binding properties for the mycotoxin ochratoxin A (OTA) in polar/protic media were prepared. Crucial to the success of these efforts was the implementation of rationally designed OTA mimics as templates and a set of novel basic and neutral functional monomers, allowing the maximization of the template–functional monomer association via ion-pairing, hydrophobic and steric interactions. MIPs prepared with a 20:1:1:3 molar ratio of cross-linking agent, template mimic, basic functional monomer and hydrophobic auxiliary monomer produced polymers with superior recognition properties compared to materials generated with other stoichiometries. Chromatographic evaluation using the OTA mimics, OTA and a set of structurally closely related compounds as analytes revealed pronounced substrate selectivity of these MIPs in polar/protic media, the templates and OTA being bound with significantly higher affinities. Complementary substrate selectivities/affinities were observed in aprotic and apolar solvents. The possibility of solvent-dependent tuning of substrate selectivity/affinity and the high binding capacity recommend the developed MIPs as promising solid-phase extraction adsorbents for clean-up and pre-concentration of OTA from various biologically relevant matrices.

Keywords: Molecular imprinting; Solid-phase extraction; Functional monomers; Mycotoxin; Ochratoxin A

1. Introduction

Ochratoxin A (OTA) is a mycotoxin of wide natural abundance produced by several species of Aspergillus (e.g., *A. ochraeus*) and Penicillium (e.g., *P. verrucosum*) fungi [1,2]. OTA can be found in various plant products such as grains, coffee beans, nuts, dried fruits, spices or wine [3,4]. Carry over effects from contaminated feed may also lead to the occurrence of residual OTA in the liver, kidney and other tissue of livestock and humans. In humans, the consumption of OTA-contaminated food exhibits nephrotoxic, teratogenic and immunosuppressive effects [5]. Apart from this, OTA is also suspected to cause the Balkan Endemic Nephropathy, a fatal kidney disease observed in rural areas in southeastern Europe (e.g., Romania, Bulgaria, Bosnia) [1]. The frequent occurrence of OTA in food has been recognized as a possible threat to human health. Consequently, many countries have set up guidelines and tolerance levels for this mycotoxin ranging from

☆ Dedicated to Professor Heinz Engelhardt on the occasion of his 65th anniversary.

* Corresponding authors. Tel.: +43-1-4277-52373/2300; fax: +43-1-4277-9523.

E-mail addresses: nmaier@anc.univie.ac.at (N.M. Maier), wolfgang.lindner@univie.ac.at (W. Lindner).

0021-9673/02/$ – see front matter
PII: S0021-9673(01)01504-7

1 to 50 μg/kg for food and 5–300 μg/kg for feed [3]. The monitoring of these tolerance levels requires selective and sensitive detection of OTA. Sample preparation for analyte enrichment and removal of interfering matrix compounds is often necessary to achieve suitable low detection limits. Clean-up and concentration steps for OTA include liquid–liquid partition [6] as well as solid-phase extraction (SPE) with reversed-phase [7,8] or ion-exchange materials [9]. Since these techniques rely on relatively unselective interactions, the resultant clean-up level may be insufficient for some challenging matrices. As a result, sample preparation with antibody-based immunoaffinity columns became increasingly popular as a selective, simple and time-saving tool for mycotoxin analysis [10–12]. These immunoaffinity adsorbents exhibit unprecedented target selectivity, but may also display some technical limitations due to their elaborous production leading to relatively high costs. More easily accessible molecularly imprinted polymers (MIPs) may represent an alternative to these established materials, as they often exhibit very selective analyte retention, and do not suffer from storage limitations and stability problems regarding organic solvents [13]. Because of these reasons, MIPs bear considerable promise to complement the repertoire of SPE materials for analyte-selective sample preparation [14–16].

Molecular imprinting is a technology to produce polymeric matrices capable of preferentially recognizing the template molecules used. Firstly, a complex between the template molecules and monomers bearing functional groups (functional monomers) is formed. The functional monomers can either be covalently linked to the template (covalent approach) or arrange themselves via non-covalent intermolecular interactions around the template molecule (non-covalent approach). The spatial assembly of these interaction sites is subsequently fixed through polymerization in the presence of a cross-linking agent. After removal of the template, binding cavities capable of recognizing and re-binding the template molecules are obtained. The binding pockets are more or less complementary to the template regarding size, shape and arrangement of the functionalities within the cavity [17–20].

For analytical applications (e.g., MIP-based SPE or MIP-based affinity assays), employing the analyte directly as an imprint molecule is problematic since a complete removal of the template from high affinity sites is generally difficult. Clearly, the slow release of the residual template (template bleeding) becomes particularly problematic when MIPs are to be used for trace analysis, because the continuous ''background'' of the template molecules released from the MIP material contaminates the processed sample and leads to false positive results and/or inaccurate quantification. Addressing this specific problem, associated with template bleeding phenomena, various groups resorted to non-covalent imprinting with analyte mimics [21–27]. Here, MIPs are generated with so-called ''dummy'' molecules which mimic shape, size and functionalities of the target analyte. Ideally, the resultant MIPs will represent binding sites showing considerable cross-selectivity for the target analytes. Co-elution of the analyte and the mimic in the course of the SPE and desorption protocols may be without consequences for the accurate determination of the analyte as long as these compounds can be distinguished in the quantification steps (e.g., chromatography). Clearly, the analyte mimic approach is also ideally suited to generate MIP-type affinity materials for analytes which can not be employed directly as templates due to pronounced toxicity, high costs and/or limited availability.

In this contribution, we describe our approach for the development of OTA selective MIP-type SPE materials. To circumvent the problems associated with the template bleeding phenomena, MIPs were prepared according to a target mimicking concept as outlined in Fig. 1. This strategy entailed the design and preparation of a series of OTA mimics as well as novel basic and neutral functional monomers (see Fig. 2) to optimize the binding affinity involving ion-pairing interactions and substrate selectivity of the resultant MIPs. The cross-selectivity of the MIP-type materials is investigated using a set of structural analogues of OTA and its mimics. Along this line, the contribution of solvents with regards to overall retention and selectivity is examined and discussed.

2. Experimental

2.1. Materials

Ethylene dimethacrylate (EDMA), 2,2′-azobisiso-

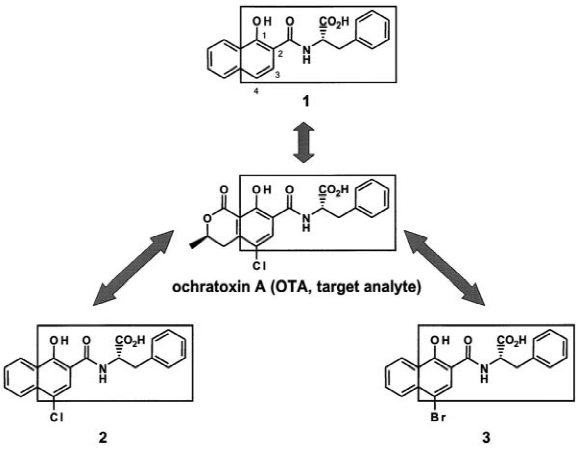

Fig. 1. Comparison of the structural features of OTA and the developed mimics.

butyronitrile (AIBN), formic acid, thionyl chloride and HPLC-grade methanol, acetonitrile, chloroform and *tert*.-butyl methyl ether were purchased from Merck (Darmstadt, Germany). 3-Aminoquinuclidine dihydrochloride and the corresponding enantiomers, 3-hyroxyquinuclidine, *n*-butyllithium (1.6 *M* in hexane), *tert*.-butyl methacrylate (*t*-Bu-MA), ammonium formate, benzyl bromide, cesium carbonate, 1-hydroxy-2-naphthoic acid, (*S*)-phenylalanine and potassium carbonate were obtained from Aldrich (Deisenhofen, Germany). OTA and ochratoxin B (OTB) were supplied from Sigma (Deisenhofen, Germany). Acetic acid (analytical-grade), bromine, *N*-ethyldiisopropylamine, *N*-hydroxysuccinimide, magnesium sulfate, methacryloyl chloride, palladium on activated carbon (5% Pd), sodium, sodium chloride, sodium hydrogencarbonate, sodium hydroxide, sodium iodide, sodium sulfite and trimethylchlorosilane were supplied by Fluka (Buchs, Switzerland). *tert*.-Butyl methacrylamide (*t*-Bu-MAA) was synthesized following a literature procedure [28]. Racemic mimics **1**–**3** and test analytes **10**–**19** were prepared at an analytical scale from the corresponding amino acids (derivatives) and acid chlorides/*O*-succinimidyl active esters following well-established Schotten–Baumann acylation protocols.

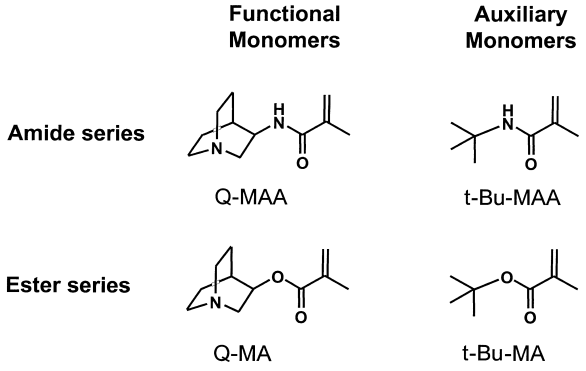

Fig. 2. Structures of the basic quinuclidine-derived functional monomers and the hydrophobic auxiliary functional monomers.

2.2. General

All reactions were carried out under strictly anhydrous conditions and under a nitrogen atmosphere. All solvents were dried by standard procedures and distilled prior to use. ^{1}H NMR spectra were acquired on a Bruker DRX 400 MHz spectrometer. The chemical shifts of the protons are given in parts per million (δ ppm) with respect to tetramethylsilane as the internal standard. Optical rotation values were recorded on a Perkin-Elmer 341 polarimeter at 25 °C. Melting points were determined with a Kofler apparatus, equipped with a Leica microscope.

2.3. Instruments

The mechanic ball mill (MM 2000) and the 25-μm sieve were supplied by Retsch (Haan, Germany). Polymers were packed with a L-6000 preparative pump from Merck (Darmstadt, Germany). Chromatographic data were acquired with a Merck-Hitachi L-7000 HPLC system (Merck Germany), consisting of a L-7150 semipreparative pump, a L-7250 autosampler and a L-7455 diode array detector. All mobile phases were composed from HPLC-grade solvents, purchased from Merck.

2.4. Syntheses of functional monomers as depicted in Fig. 2

2.4.1. Racemic, (S)- and (R)-quinuclidin-3-yl methacrylamide (Q-MAA)

A 6 g amount of of racemic or enantiomerically pure 3-aminoquinuclidine dihydrochloride (30 mmol) was dissolved in methanol (50 ml) and a freshly prepared methoxide solution (1.38 g of sodium in 25 ml methanol, 60 mmol, 2 equivalents)

was added. After addition of diethyl ether (25 ml) the suspension was allowed to stand for 2 h at 4 °C. The precipitated sodium chloride was removed by filtration. The filtrate was evaporated and the residue dried in high vacuum at ambient temperature. The resultant amine was dissolved in chloroform (60 ml) and cooled to 0 °C. A solution of methacryloyl chloride (6.30 g, 60 mmol, 2 equivalents) in chloroform (60 ml) was added and stirred for 12 h at ambient temperature. The volatiles were evaporated and the residue dried in high vacuum. The solid was dissolved in chloroform (100 ml), transferred into a separating funnel and washed with 2 *M* aqueous sodium hydroxide (1×100 ml) and half-saturated sodium chloride solution (2×100 ml). After drying ($MgSO_4$), the solvent was removed under reduced pressure at ambient temperature, giving white wax-like crystals which were dried in high vacuum. Yield: 4.47 g, 23 mmol, 76%. ^{1}H NMR (C^2HCl_3) δ 1.7 (m, 4H), 1.95 (m, 4H), 2.45–2.55 (m, 1H), 2.75–2.95 (m, 4H), 3.3–3.5 (m, 1H), 3.9–4.1 (m, 1H), 5.35 (s, 1H), 5.7 (s, 1H), 5.9 (b, 1H). (*R*)-Q-MAA: $[\alpha]_{589}^{25} = +29.0$ ($c = 1.0$, methanol), (*S*)-Q-MAA: $[\alpha]_{589}^{25} = -30.6$ ($c = 1.0$, methanol).

*2.4.2. Racemic quinuclidin-3-yl methacrylate (*Q-MA*)*

3-Hydroxy quinuclidine (2.0 g, 15.7 mmol) was dissolved in tetrahydrofuran (50 ml). The solution was cooled to −80 °C (acetone–dry ice mixture). Then 10.8 ml (17.3 mmol, 1.1 equivalents) of a 1.6 *M* solution of *n*-butyllithium in hexane was added dropwise via a syringe. The reaction mixture was allowed to warm up to ambient temperature and a solution of methacryloyl chloride (1.85 ml, 17.3 mmol. 1.1 equivalents) in tetrahydrofuran (10 ml) was added via a dropping funnel. The reaction mixture was stirred for 30 min. After evaporation of the solvent, the residue was dissolved in ethyl acetate (50 ml). The solution was washed with 0.5 *M* aqueous sodium hydroxide (2×50 ml) and brine (2×50 ml). After drying ($MgSO_4$), the solvent was evaporated at ambient temperature and the residue dried in high vacuum. The resultant yellow oil was purified by column chromatography on silica with chloroform–methanol = 1:1 as the eluent. Yield: 2.29 g, 11.7 mmol, 74%. ^{1}H NMR (C^2HCl_3) δ 1.43 (m, 1H), 1.6 (m, 1H), 1.7 (m, 1H), 1.86 (m, 1H), 1.95 (s, 3H), 2.05 (m, 1H), 2.15 (b, 1H), 2.68–2.95 (m, 4H), 3.25 (m, 1H), 4.88 (m, 1H), 5.58 (s, 1H), 6.15 (s, 1H).

2.5. Syntheses of analyte mimics (see Fig. 3)

*2.5.1. (S)-N-[(1-Hydroxy)-2-naphthoyl]-phenylalanine (***1***)*

*2.5.1.1. Benzyl-(1-benzyloxy)-2-naphthoate (***5a***)*

1-Hydroxy-2-naphthoic acid (9.4 g, 50 mmol), potassium carbonate (27.65 g, 0.2 mol, 4 equivalents), cesium carbonate (1.63 g, 5 mmol, 0.1 equivalents) and benzyl bromide (15 ml, 0.125 mol, 2.5 equivalents) were dissolved in dimethylformamide (150 ml). The reaction mixture was heated with stirring for 2 h at 70–80 °C. The progress of the reaction was followed by TLC analysis [light petroleum (b.p. 40–60 °C)–ethyl acetate = 10:1 on silica]. The mixture was poured into ice water and extracted with ethyl acetate (2×500 ml). The combined organic layers were washed with brine (3×500 ml) and dried ($MgSO_4$). The solvent was evaporated and the residue dried in high vacuum to give a white waxy solid. Yield: 17.41 g, 47.3 mmol, 94%. ^{1}H NMR (C^2HCl_3) δ 5.14 (s, 2H), 5.40 (s, 2H), 7.29–7.53 (m, 10H), 7.57 (t, 1H), 7.63 (d, 1H), 7.85 (d, 1H), 7.92 (d, 1H), 8.25 (d, 1H).

*2.5.1.2. 1-Benzyloxy-2-naphthoic acid (***6a***)*

A 17.4 g amount of **5a** was dissolved in methanol (500 ml). Then 60 ml of a 3.6 *M* aqueous sodium hydroxide solution was added and the mixture was refluxed for 4 h. The progress of the reaction was followed by TLC analysis (light petroleum–ethyl acetate = 10/1 on silica). The volatiles were evaporated and the residue dissolved in water (400 ml). The solution was extracted with diethyl ether (4× 150 ml). The aqueous phase was then acidified with 2 *M* aqueous hydrochloric acid to pH 1–2. The formed precipitate was isolated by filtration and dried under vacuum over solid sodium hydroxide to give a white solid. Yield: 12.61 g, 45.3 mmol, 95%. ^{1}H NMR (C^2HCl_3) δ 5.25 (s, 2H), 7.45 (m, 3H), 7.55 (d, 2H), 7.63 (m, 2H), 7.74 (d, 1H), 7.92 (d, 1H), 8.10 (d, 1H), 8.25 (d, 1H). m.p.: 126–129 °C.

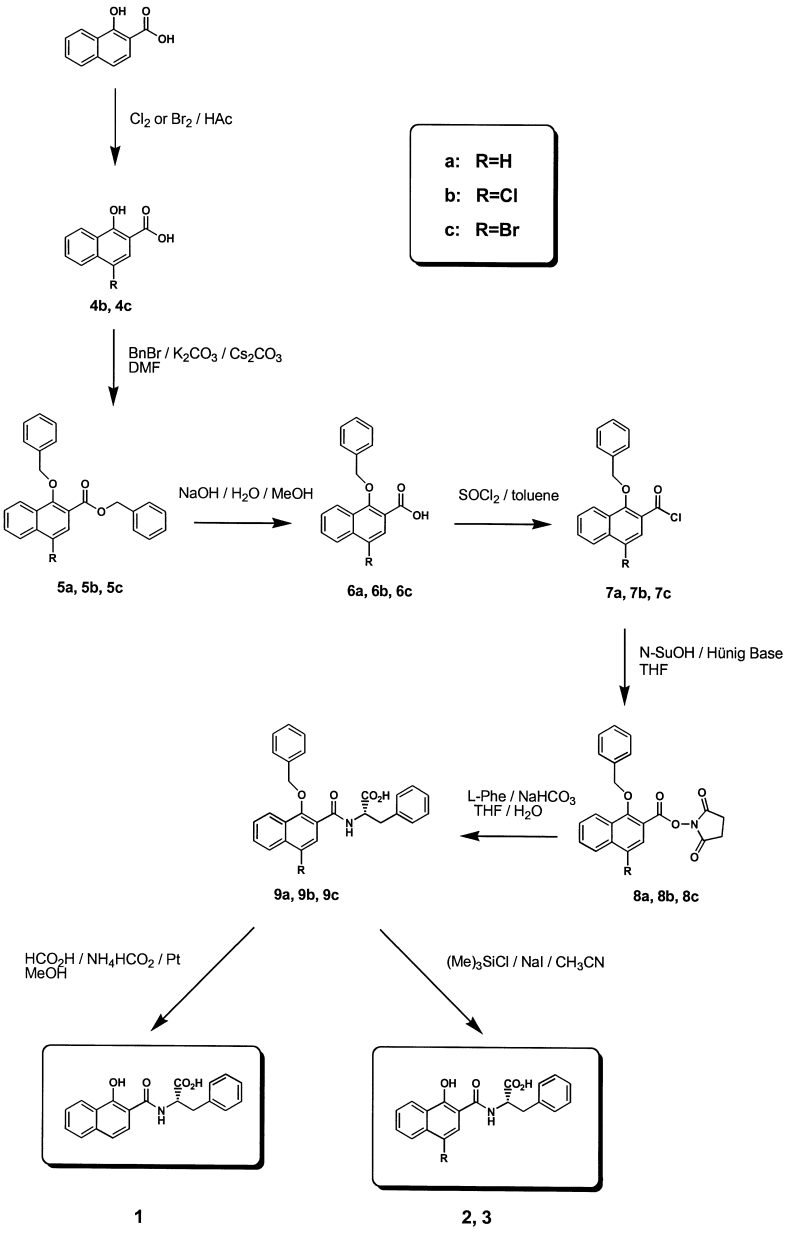

Fig. 3. Synthetic routes for the preparation of the OTA mimics.

*2.5.1.3. 1-Benzyloxy-2-naphthoyl chloride (***7a***)*

To a solution of **6a** (11.14 g, 40 mmol) in toluene (100 ml), freshly distilled thionyl chloride (7.14 g, 60 mmol, 1.5 equivalents) and dimethylformamide (200 μl) were added. The mixture was refluxed for 3 h. The progress of the reaction was monitored by TLC analysis (chloroform–methanol = 5:1 on silica). Then, the volatiles were evaporated under reduced pressure to give brown crystals. Yield: 11.87 g, 40 mmol, 100%. ^{1}H NMR ($C^{2}HCl_3$) δ 5.25 (s, 2H),

7.45 (m, 3H), 7.53 (d, 2H), 7.63 (m, 2H), 7.73 (d, 2H), 7.93 (d, 1H), 8.10 (d, 1H), 8.25 (d, 1H). m.p.: 112–114 °C.

*2.5.1.4. O-Succinimidyl-(1-benzyloxy)-2-naphthoate (**8a**)*

N-Hydroxysuccinimide (2.91 g, 25 mmol, 1.25 equivalents) and *N*-ethyldiisopropyl amine (4.4 ml, 25 mmol, 1.25 equivalents) were dissolved in tetrahydrofuran (50 ml). Under ice cooling, **7a** (5.94 g, 20 mmol), dissolved in tetrahydrofuran (65 ml), was added via a dropping funnel. The progress of the reaction was followed by TLC analysis (ethyl acetate on silica). After 12 h, ethyl acetate (250 ml) was added and the resultant organic phase was washed with 2 *M* aqueous hydrochloric acid (1×100 ml), 5% sodium hydrogencarbonate (2×100 ml) and brine (3×100 ml). The organic phase was dried ($MgSO_4$) and the volatiles were removed under reduced pressure to give off-white crystals. Yield: 6.87 g, 18.3 mmol, 91%. ^{1}H NMR (C^2HCl_3) δ 2.92 (s broad, 4H), 5.25 (s, 2H), 7.40 (m, 3H), 7.56 (m, 3H), 7.65 (t, 1H), 7.79 (d, 1H), 7.88 (d, 1H), 8.02 (d, 1H), 8.25 (d, 1H). m.p.: 127–129 °C.

*2.5.1.5. (S)-N-[(1-Benzyloxy)-2-naphthoyl]-phenylalanine (**9a**)*

A sample of **8a** (2.72 g, 7.2 mmol) was dissolved in tetrahydrofuran (250 ml). Then a solution of (*S*)-phenylalanine (1.80 g, 10.8 mmol, 1.5 equivalents) and sodium hydrogencarbonate (4.57 g, 54 mmol, 7.5 equivalents) in water (250 ml) was prepared. The solutions were mixed and stirred for 12 h at room temperature. The progress of the reaction was monitored by TLC analysis (chloroform–methanol=5:1 on silica). The volatiles were removed under reduced pressure. The residue was dissolved in water (100 ml) and the solution was acidified with 2 *M* aqueous hydrochloric acid (pH 1–2). The product was extracted with ethyl acetate (2×100 ml). The combined organic layers were washed with brine (2×100 ml) and dried ($MgSO_4$). Removal of the solvent and drying in high vacuum gave a brown foam. Yield: 2.93 g, 6.9 mmol, 95%. ^{1}H NMR (C^2HCl_3) δ 3.0 (m, 1H), 3.30 (m, 1H), 4.90–5.08 (m, 3H), 7.08 (m, 2H), 7.18 (m, 3H), 7.38 (m, 5H), 7.52 (t, 1H), 7.58 (t, 1H), 7.70 (d, 1H), 7.87 (d, 1H), 8.12 (m, 2H), 8.55 (d, 2H). m.p.: 47–50 °C. $[\alpha]_{589}^{25} = -37.9$ ($c=1.0$, methanol).

*2.5.1.6. (S)-N-[(1-Hydroxy)-2-naphthoyl]-phenylalanine (**1**)*

A sample of **9a** (3.5 g, 8.2 mmol) was dissolved in methanol (100 ml). Ammonium formate (6 g, 95 mmol, 11.5 equivalents) and formic acid (2 ml, 50 mmol, 6 equivalents) were added. Then palladium on activated carbon (0.5 g, 5% Pd), suspended in methanol, was added to the solution. The mixture was refluxed for 3 h. The progress of the reaction was monitored by TLC analysis (chloroform–methanol=5:1 on silica). The catalyst was removed by filtration, the solvent was evaporated and the residue was taken into water (150 ml). The filtrate was acidified with 2 *M* sulfuric acid (pH 1–2). The mixture was extracted with ethyl acetate (50 ml). The organic phase was washed with brine (2×50 ml) and water (2×50 ml) and dried ($MgSO_4$). The volatiles were removed under reduced pressure and the residue carefully dried in vacuum to give brown crystals. Yield: 2.65 g, 7.9 mmol, 96%. ^{1}H NMR (C^2HCl_3) δ 3.3–3.48 (m, 2H), 5.2 (m, 1H), 6.74 (d, 1H), 7.18–7.4 (m, 7H), 7.45 (t, 1H), 7.52 (t, 1H), 7.77 (d, 1H), 8.45 (d, 1H). m.p.: 123–125 °C. $[\alpha]_{589}^{25} = -36.5$ ($c=1.0$, methanol).

*2.5.2. (S)-N-[(4-Chloro-1-hydroxy)-2-naphthoyl]-phenylalanine (**2**)*

OTA mimic **2** was prepared following essentially the same synthetic route as described for **1** using **4b** as the starting material. However, *O*-debenzylation of **9b** was performed using a silicon-based ether cleavage protocol [29] as hydrogenation gave rise to extensive dehalogenation.

*2.5.2.1. 4-Chloro-1-hydroxy-2-naphthoic acid (**4b**)*

This compound was prepared following a literature procedure [30]. White crystals. Yield: 79%. ^{1}H NMR (C^2HCl_3) δ 3.74 (s broad, 1H), 7.68 (t, 1H), 7.83 (t, 1H), 8.14 (d, 1H), 8.22 (d, 1H), 8.38 (d, 1H). m.p.: 202–204 °C.

*2.5.2.2. Benzyl-(4-chloro-1-benzyloxy)-2-naphthoate (**5b**)*

White solid. Yield: 91%. ^{1}H NMR (C^2HCl_3) δ 5.1 (s, 2H), 5.4 (s, 2H), 7.36 (m, 6H), 7.45 (m, 4H), 7.7

(t, 1H), 7.57 (t, 1H), 8.05 (s, 1H), 8.25 (m, 2H). m.p.: 80–81 °C.

*2.5.2.3. 4-Chloro-1-benzyloxy-2-naphthoic acid (**6b**)*

White solid. Yield: 92%. ^{1}H NMR (C^2HCl_3) δ 5.25 (s, 2H), 7.45 (m, 3H), 7.55 (m, 2H), 7.67 (t, 1H), 7.78 (t, 1H), 8.2 (s, 1H), 8.29 (d, 1H), 8.34 (d, 2H). m.p.: 158–160 °C.

*2.5.2.4. 4-Chloro-1-benzyloxy-2-naphthoyl chloride (**7b**)*

White solid. Yield: 100%. ^{1}H NMR (C^2HCl_3) δ 5.14 (s, 2H), 7.45 (m, 3H), 7.55 (m, 2H), 7.62 (t, 1H), 7.8 (t, 1H), 8.16 (s, 1H), 8.29 (d, 2H). m.p.: 124–125 °C.

*2.5.2.5. O-Succinimidyl-(4-chloro-1-benzyloxy)-2-naphthoate (**8b**)*

White crystals. Yield: 92%. ^{1}H NMR (C^2HCl_3) δ 2.95 (s broad, 4H), 5.23 (s, 2H), 7.40 (m, 3H), 7.55 (m, 2H), 7.61 (t, 1H), 7.77 (t, 1H), 8.14 (s, 1H), 8.29 (d, 2H). m.p.: 141–142 °C.

*2.5.2.6. (S)-N-[(4-Chloro-1-benzyloxy)-2-naphthoyl]-phenylalanine (**9b**)*

Colorless glassy solid. Yield: 90%. ^{1}H NMR (C^2HCl_3) δ 3.01 (m, 1H), 3.30 (m, 1H), 4.91 (d, 1H), 4.99 (m, 1H), 5.04 (m, 1H), 7.07 (d, 2H), 7.20 (m, 4H), 7.37 (m, 5H), 7.58 (t, 1H), 7.68 (t, 1H), 8.15 (d, 1H), 8.25 (d, 1H), 8.43 (d, 2H). $[\alpha]_{589}^{25} = -33.1$ ($c = 1.0$, methanol).

*2.5.2.7. (S)-N-[(4-Chloro-1-hydroxy)-2-naphthoyl]-phenylalanine (**2**)*

A 0.74 g amount of **9b** (2 mmol) was dissolved in acetonitrile (10 ml). The solution was cooled to 0 °C and then sodium iodide (0.60 g, 4 mmol, 2 equivalents) and trimethylchlorosilane (0.50 ml, 4 mmol, 2 equivalents) were added. The reaction mixture was stirred for 1 h at ambient temperature. A mixture of ethyl acetate (100 ml) and ice cold 5% sulfuric acid (50 ml) was added followed by solid sodium sulfite (3.0 g). After washing of the organic phase with a 10% aqueous sodium chloride solution (2×100 ml), the product was extracted with 100 ml of a 1 *M* aqueous sodium hydroxide solution. The aqueous phase was acidified with a 5% sulfuric acid (pH 1–2) and the product extracted with ethyl acetate (2×100 ml). The combined organic layers were washed with a 10% aqueous sodium chloride solution (2×100 ml) and dried ($MgSO_4$). The solvent was evaporated and the residue was dried in high vacuum to give brownish crystals. Yield: 0.67 g, 1.8 mmol, 90%. ^{1}H NMR (C^2HCl_3) δ 3.25–3.42 (m, 2H), 5.15 (m, 1H), 6.65 (d, 1H), 7.17–7.42 (m, 6H), 7.6 (t, 1H), 7.7 (t, 1H), 8.15 (d, 1H), 8.45 (d, 1H). m.p.: 168–170 °C. $[\alpha]_{589}^{25} = -66.5$ ($c = 1.0$, methanol).

*2.5.3. (S)-N-[(4-Bromo-1-hydroxy)-2-naphthoyl]-phenylalanine (**3**)*

OTA mimic **3** was prepared following essentially the same synthetic route as outlined for **1** using **4c** as the starting material. *O*-Debenzylation of **9c** was performed using the silicon-based ether cleavage protocol described for **9b**.

*2.5.3.1. 4-Bromo-1-hydroxy-2-naphthoic acid (**4c**)*

This compound was prepared following a literature procedure [30]. Yellowish crystals. Yield: 73%. ^{1}H NMR (C^2HCl_3) δ 7.62 (t, 1H), 7.76 (t, 1H), 8.14 (d, 1H), 8.42 (d, 1H), 8.60 (s, 1H). m.p.: 248–251 °C.

*2.5.3.2. Benzyl-(4-bromo-1-benzyloxy)-2-naphthoate (**5c**)*

White solid. Yield: 95%. ^{1}H NMR (C^2HCl_3) δ 5.12 (s, 2H), 5.39 (s, 2H), 7.35 (t, 6H), 7.44 (d, 4H), 7.56 (t, 1H), 7.69 (t, 1H), 8.24 (m, 3H). m.p.: 83–84 °C.

*2.5.3.3. 4-Bromo-1-benzyloxy-2-naphthoic acid (**6c**)*

Off-white crystals. Yield: 100%. ^{1}H NMR (C^2HCl_3) δ 5.25 (s, 2H), 7.46 (m, 3H), 7.53 (m, 2H), 7.69 (t, 1H), 7.78 (t, 1H), 8.30 (m, 2H), 8.42 (s, 1H). m.p.: 170–175 °C.

*2.5.3.4. 4-Bromo-1-benzyloxy-2-naphthoyl chloride (**7c**)*

Slightly yellowish solid. Yield: 96%. ^{1}H NMR (C^2HCl_3) δ 5.15 (s, 2H), 7.43 (m, 3H), 7.55 (d, 2H), 7.64 (t, 1H), 7.80 (t, 1H), 8.27 (t, 2H), 8.38 (s, 1H). m.p.: 131–133 °C.

*2.5.3.5. O-Succinimidyl-(4-bromo-1-benzyloxy)-2-naphthoate (***8c***)*

Crystalline white solid. Yield: 83%. ^{1}H NMR (C^2HCl_3) δ 2.92 (s broad, 4H), 5.22 (s, 2H), 7.39 (m, 3H), 7.54 (m, 2H), 7.60 (t, 1H), 7.76 (t, 1H), 8.28 (m, 2H), 8.35 (s, 1H). m.p.: 151–154 °C.

*2.5.3.6. (S)-N-[(4-Bromo-1-benzyloxy)-2-naphthoyl]-phenylalanine (***9c***)*

White crystals. Yield: 100%. ^{1}H NMR (C^2HCl_3) δ 3.01 (m, 1H), 3.30 (m, 1H), 4.91 (d, 1H), 4.99 (m, 1H), 5.04 (m, 1H), 7.07 (d, 2H), 7.20 (m, 4H), 7.37 (m, 5H), 7.58 (t, 1H), 7.68 (t, 1H), 8.15 (d, 1H), 8.25 (d, 1H), 8.43 (d, 2H). m.p.: 153–156 °C. $[\alpha]_{589}^{25} = -30.4$ ($c = 1.0$, methanol).

*2.5.3.7. (S)-N-[(4-Bromo-1-hydroxy)-2-naphthoyl]-phenylalanine (***3***)*

Colorless crystals. Yield: 84%. ^{1}H NMR (C^2HCl_3) δ 2.06 (s, 1H), 3.30 (m, 1H), 3.38 (m, 1H), 5.14 (m, 1H), 6.69 (t, 1H), 7.24 (t, 2H), 7.32 (m, 3H), 7.51 (s, 1H), 7.59 (t, 1H), 7.72 (t, 1H), 8.12 (d, 1H), 8.44 (d, 1H). m.p.: 71–73 °C. $[\alpha]_{589}^{25} = -63.7$ ($c = 0.93$, methanol).

2.6. Evaluation of enantiomeric excess of the analyte mimics **1**–**3**

Enantiomeric excess (ee) was established by high-performance liquid chromatography (HPLC) using a quinine-derived chiral stationary phase (6-OH-*t*-Bu-CQN, 150×4 mm I.D.) [31]: mobile phase: methanol–1 *M* ammonium acetate (80:20, v/v), $pH_a = 6.0$; flow: 1 ml/min; detection: UV 254 nm; column temperature: 30 °C; retention factors: OTA mimic **1**: $k_R = 4.84$, $k_S = 6.89$; OTA mimic **2**: $k_R = 6.92$, $k_S = 16.83$; OTA mimic **3**: $k_R = 8.29$; $k_S = 20.24$. For all analytes, ee values of >95% were established and no chemical impurities could be detected under these conditions.

2.7. General procedure for the preparation of the MIPs

In a screwcap centrifugation tube, the template molecules (**1**, **2** or **3**), EDMA and the corresponding functional monomers (Q-MAA, Q-MA, *t*-Bu-MAA and *t*-Bu-MA) were mixed in the molar ratios given in Table 1. After addition of AIBN (40 mg, 0.25 mmol) and chloroform (5.6 ml) the solution was purged with nitrogen for 5 min. The tubes were sealed and kept at 65 °C for 24 h to achieve polymerization. The vials were crushed and the formed polymer rods were ground using a mechanical ball mill. The resultant materials were suspended in acetone and driven through a 25-μm sieve with gentle brushing. Fines were removed by repeated sedimentation steps in acetone containing 4% acetic acid. The corresponding non-imprinted control poly-

Table 1
Composition of the polymerization mixtures used for the preparation of the MIPs **P1**–**P8**[a]

Polymer	Individual components of the polymerization mixtures (mmol)							
	Cross-linker	Functional monomer[b]				Template[c]		
	EDMA	Q-MAA	Q-MA	*t*-Bu-MAA	*t*-Bu-MA	**1**	**2**	**3**
P1[d]	20	4	–	–	–	1	–	–
P2[d]	20	2	–	2	–	1	–	–
P3[d]	20	1	–	3	–	1	–	–
P4	20	1	–	3	–	–	1	–
P5	20	1	–	3	–	–	–	1
P6[d]	20	1 (*S*)	–	3	–	1	–	–
P7[d]	20	1 (*R*)	–	3	–	1	–	–
P8[d]	20	–	1	–	3	1	–	–

[a] Chloroform (5.6 ml) was employed as porogenic solvent, polymerization was performed under nitrogen at 65 °C for 24 h.
[b] See Fig. 2 for the structures of the respective functional monomers.
[c] See Fig. 1 for structures of the OTA mimics.
[d] corresponding non-imprinted control polymers (NIPs) were prepared under identical conditions without the respective templates.

mers (NIPs) were prepared as described above, but in absence of the template molecules.

2.8. Chromatographic evaluation of the MIPs

The MIPs were slurry packed in methanol into 125×4 mm I.D. stainless steel HPLC columns using a preparative HPLC pump (Merck L-6000) in the constant pressure mode at 10 MPa for about 30 min. The columns were extensively washed with a methanol–acetic acid (95:5, v/v) mixture overnight at a flow-rate of 1 ml/min in order to remove the template from the polymer matrix. Chromatographic experiments were performed on a LaChrom L-7000 HPLC system from Merck. The flow-rate was 1 ml/min and the column temperature 30 °C (controlled with a thermostat). Detection was carried out at $\lambda = 254$ nm. Acetone was used as void volume marker. For chromatographic evaluation, 20 μl of a 1 m*M* solution was injected.

2.9. Determination of binding capacity by frontal analysis

The binding capacity of imprinted polymer **P3** for OTA mimic **1** was determined via frontal analysis as described in the literature [32]. For this purpose, a 50×4 mm I.D. stainless steel HPLC column was packed with particles of **P3**. To ensure complete removal of the template, the column was extensively washed with a methanol–acetic acid (95:5, v/v) mixture, then with a methanol–triethylamine (99:1, v/v) mixture and finally with methanol. Frontal analysis runs were performed in triplicate at 30 °C and a flow-rate of 0.25 ml/min. Breakthrough of **1** was detected at $\lambda = 370$ nm, and acetone was used as non-retained void volume marker.

3. Results and discussion

The widespread occurrence of OTA in agricultural products and in animal and human tissue poses a considerable challenge in context with sample pretreatment. The heterogeneity in terms of the concentration range and interfering matrix compounds demands highly selective extraction and enrichment of this mycotoxin to facilitate and speed up the determination and quantification. To be competitive with established SPE materials, suitable MIPs have to fulfil a number of requirements: (i) they have to show considerable affinity and selectivity towards the target analyte; (ii) the molecular recognition principle has to be compatible with a wide range of solvent systems (apolar and polar/protic media) for broad applicability; (iii) the binding capacities must be high.

3.1. Design and synthesis of OTA mimics to be used as templates

Pronounced toxicity, limited availability and in particular the problems associated with the direct use of the target analyte as template (''template bleeding'') precluded the direct use of OTA for the preparation of selective MIP-type SPE materials. For these reasons, we decided to generate MIPs with structural mimics of OTA as templates to produce affinity materials displaying binding cavities with cross-selectivity also for the mycotoxin. Suitable mimics have to resemble OTA in terms of size, shape, functionality, stereochemistry and lipophilicity. Furthermore, from a practical viewpoint, the mimics have to be easily accessible in amounts of several grams. To meet these criteria, we designed and synthesized a series of three different OTA mimics, the structures of which are depicted in Fig. 1. These mimics comprise the phenol functionality, the amide group and the phenylalanine amino acid side chain of the mycotoxin in correct spatial arrangement and stereochemistry. To further enhance the structural similarity with OTA, chlorine and bromine were introduced at the 4-position of the naphthol ring in compounds **2** and **3**, respectively. Synthetically, the preparation of the mimics was based on commercially readily available starting materials and involved six and seven steps (see Fig. 3). The optimized synthetic pathways gave access to chemically and enantiomerically pure OTA mimics in 10-g amounts with excellent overall yields (>50%), avoiding time-consuming purification steps of intermediates.

3.2. Synthesis of novel functional monomers for promoting intermolecular ion-pairing and hydrophobic template–functional monomer interactions

The structural features of the OTA mimics suggest that these molecules may be capable of forming intermolecular complexes with appropriate functional monomers via a variety of non-covalent intermolecular interactions. The acidic functionalities of the OTA mimics shall effectively interact with functional monomers offering basic centers for ion-pairing and hydrogen bonding interactions. The amide bond linking the naphthol unit with the amino acid may also be able to bind to the functional monomers by hydrogen bonding and dipole–dipole interactions. The aromatic domains can provide structural elements that stabilize intermolecular complexes via $\pi-\pi$ interactions and hydrophobic association.

Guided by these considerations, a set of well-established functional monomers, including methacrylic acid, methacrylamide, hydroxyethyl methacrylate and 4-vinylpyridine as well as combinations of these systems were initially selected for exploratory imprinting studies. Along this line, various solvents (methanol, chloroform, cyclohexanone, dodecanol) were tested as porogens to enhance the interactions of the ochratoxin mimics and these functional monomers. In all these cases, EDMA was employed as cross-linking agent and polymerization was performed thermally using AIBN as the initiator. To identify MIP candidates compatible with polar/protic media, the resultant polymers were evaluated chromatographically using methanol–acetic acid (95:5, v/v). However, neither of these MIPs showed significant levels of selective binding of OTA mimics or OTA (data not shown).

These somewhat disappointing results prompted us to develop novel functional monomers that would specifically address the structural features of OTA and its mimics. With the intention of strengthening ion-pairing interactions with the acidic templates in polar/protic media, strongly basic functional monomers were designed (see Fig. 2). Moreover, we felt that an enhancement of the rigidity and the hydrophobic nature of the functional monomers might add to their molecular recognition potential for the templates. To provide monomers combining strong basicity and high rigidity together with pronounced hydrophobicity, quinuclidine-type methacrylamide (Q-MAA) and methacrylate (Q-MA) were prepared. The intrinsic chirality of these compounds was also expected to provide a means to tune the stability of template–functional monomer complexes.

Additionally, *tert.*-butyl methacrylamide and *tert.*-butyl methacrylate (*t*-Bu-MAA and *t*-Bu-MA, see Fig. 2) were implemented as co-functional monomers. These auxiliary monomers are similar to the corresponding quinuclidine monomers in their steric requirements, but lack the basic centers, and therefore should allow to control the hydrophobic contributions to template–functional monomer association.

3.3. Stoichiometry of imprinting

With this set of novel functional monomers and OTA mimics as templates in hand, further attempts for the preparation of OTA selective MIPs were carried out. MIPs were prepared following the well-established non-covalent imprinting protocol, with formulations comprising cross-linking agent, functional monomer(s) and template in 20:4:1 molar amounts [33]. To maximize the stability of the template–functional monomer complexes, all MIPs were prepared using chloroform as an ion-pair and hydrogen bond preserving porogenic solvent. Polymerization was initiated with AIBN and performed under thermal conditions.

Exploratory imprinting experiments were carried out using OTA mimic **1** as the template (see Fig. 1). Polymers produced with Q-MAA as single functional monomer (**P1**) displayed both considerable affinity and enantioselectivity for the imprint molecule under chromatographic conditions using methanol–acetic acid (95:5, v/v) as the mobile phase. The levels of enantioselectivity observed for MIPs imprinted with single enantiomer templates provided a direct measure for the ''quality'' of the generated binding sites [17]. Thus, MIPs displaying high levels of enantioselectivities for the templates must possess binding cavities with pronounced three-dimensional complementarity, capable of not only recognizing functional and electronic, but also stereochemical and shape-related features of the imprint molecule and structurally related compounds.

These results demonstrated the potential of the novel quinuclidine-derived functional monomer to

create binding sites capable of selective template re-binding from polar/protic media. However, the overall retention for the template was exceedingly strong also with the corresponding NIPs, indicating substantial contributions of non-selective binding increments. Thus, to attenuate non-selective binding and/or to promote more selective recognition properties, a new series of MIPs was prepared in which the basic Q-MAA was stepwise replaced by the neutral *t*-Bu-MAA. As can be seen in Fig. 4, the addition of this non-basic co-functional monomer to the polymerization mixture had favorable effects on the chromatographic performance of these MIPs. Thus, employing EDMA, Q-MAA, *t*-Bu-MAA and the template in a 20:2:2:1 molar ratio (**P2**) led to a reduction of the overall retention by 50% but to an increase in enantioselectivity for **1** from $\alpha = 1.25$ to 1.31. The improvement of enantioselectivity and suppression of non-selective retention were even more pronounced when Q-MAA and *t*-Bu-MAA were implemented in a 1:3 ratio (**P3**).

Obviously, the formation of the pre-polymerization complex between the acidic template and the basic Q-MAA is dominated by ion-pairing interactions and occurs in a stoichiometric fashion. Any excess of basic functional monomer facilitates the generation of additional but mismatched interaction centers, which compromise the overall retention and selectivity by non-selective electrostatic forces. In contrast, employing template and Q-MAA in 1:1 ratio seems to produce so-called non-covalent stoichiometric imprinted MIPs, which show molecular recognition properties superior to conventional non-covalent imprinted polymers. These advantages include thermodynamically rather homogenous binding sites and conservation of the majority of active binding centers on elution of the template, allowing for a high re-binding capacity for the template and structurally related molecules. In order to preserve these intrinsic advantages, all the polymers discussed in the following sections were prepared using Q-MAA and *t*-Bu-MAA in a 1:3 molar ratio.

3.4. Influence of analyte mimic

Generally, the level of MIP cross-selectivity observed between a given analyte and the template species is related to the degree of structural and electronic similarity that exists between those molecules. In order to establish the influence of the

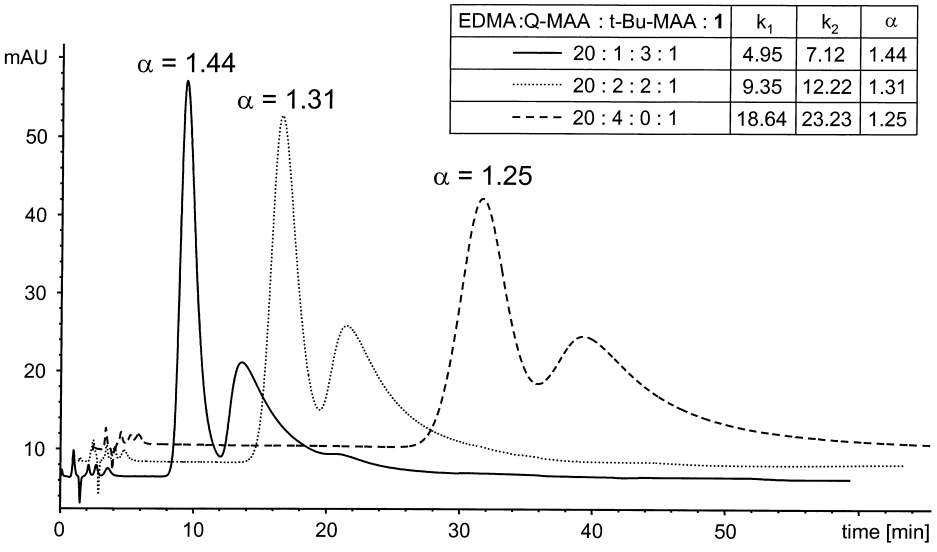

Fig. 4. Influence of the relative molar amounts of the amide-type functional and auxiliary monomers on the retention behavior and enantioselectivity on MIPs (**P1**–**P3**) imprinted with mimic **1**. Chromatographic conditions: MIP columns: 125×4 mm I.D., mobile phase: methanol–acetic acid (95:5, v/v), flow-rate: 1 ml/min, temperature: 30 °C, detection: 254 nm. analyte: racemic **1**. In all cases the (*S*)-enantiomer was more strongly retained.

template structure on the OTA selectivity, MIPs **P4** and **P5** were prepared replacing **1** with **2** and **3** as templates (see Table 1). As it is evident from Fig. 1, mimics **2** and **3** bear closer structural resemblance to OTA than **1** due to the presence of chlorine and bromine in position 4, respectively. Thus, it was expected that **P4** and **P5** would display higher affinity for OTA than **P3**.

The chromatographic evaluation of these polymers revealed considerable cross-selectivity of the binding sites, indicated by the capability of enantioselective recognition of racemic mixtures of **1**, **2** and **3**. In all cases, the enantioselectivity was most pronounced for the compound incorporated as the template during polymerization, providing evidence for very subtle differences in binding site geometries of **P3**, **P4** and **P5** (see Table 2). This is in accordance with previous findings of several other groups [21,23,24,34]. Although **P4** and **P5** displayed some enhancement in terms of OTA binding, the improvements achieved in retention were rather incremental. These findings suggest that the chlorine and bromine containing templates **2** and **3** do not shape superior binding sites as compared to the smaller template **1**. For these reasons, all further MIPs were generated with the synthetically less elaborate OTA mimic **1**.

3.5. Stereochemistry of the functional monomer

The basic functional monomer Q-MAA and the acidic OTA mimics used as templates in MIP preparation are chiral molecules. Employing racemic Q-MAA as a functional monomer gives rise to the formation of diastereomeric ion-pairs in the pre-polymerization mixtures with different thermodynamic stabilities. Consequently, the incorporation of these associates into the polymeric matrix might create diastereomeric binding cavities with enantioselective re-uptake potential of the templates and structurally related chiral compounds.

Concerning the performance of MIPs, imprinting processes involving chiral template–functional monomer species may lead to different outcomes: (i) Binding pockets shaped from intrinsically chiral components may show improved substrate selectivity due to a more pronounced spatial pre-organization of the interaction sites. (ii) The presence of mixtures of diastereomeric pre-polymerization complexes also may compromise the overall affinity of imprinted polymers by promoting binding site heterogeneity and thus leading to decreased stereoselectivity.

To assess which of these mechanisms would control the overall binding affinity of our MIP systems, we prepared **P6** and **P7** from enantiomerically pure Q-MAA monomers and template **1** (see Table 1). A comparison of the chromatographic retention data of these polymers with those of **P3**, produced with racemic Q-MAA, is given in Table 3. In terms of enantioselectivity, **P6** prepared with the (*S*)-Q-MAA showed for racemic **1**, **2**, **3** and OTA a very similar behavior to **P3**. **P7** prepared in presence of (*R*)-Q-MAA appears to be slightly inferior relative

Table 2
Molecular recognition properties of polymers **P3**–**P5** prepared using OTA mimics **1**, **2** and **3** as templates[a]

Analyte	Polymer									
	NIP	**P3**[c]			**P4**[d]			**P5**[e]		
	k	k_2	α[f]	IF[g]	k_2	α	IF	k_2	α	IF
1[b]	4.78	7.12	1.44	1.49	6.00	1.22	1.26	6.15	1.21	1.29
2[b]	5.02	6.20	1.20	1.24	7.08	1.35	1.41	7.26	1.33	1.45
3[b]	5.55	6.51	1.14	1.17	7.83	1.34	1.41	8.28	1.36	1.49
OTA	5.18	5.66	–	1.09	5.80	–	1.12	6.00	–	1.16

[a] For the chromatographic conditions see Fig. 4.
[b] Analytes **1**–**3** were employed as racemic mixtures.
[c] Mimic **1** as template.
[d] Mimic **2** as template.
[e] Mimic **3** as template.
[f] Enantioselectivity value ($\alpha = k_2/k_1$).
[g] Imprinting factor ($IF = k_{MIP}/k_{NIP}$).

Table 3
Influence of stereochemistry of the basic functional monomer Q-MAA on the molecular recognition properties of polymers **P3**, **P6** and **P7** imprinted with OTA mimic **1**[a]

Analyte	Polymer											
	NIP	**P3**			NIP	**P6**			NIP	**P7**		
	k	k_2	α[c]	IF[d]	k	k_2	α	IF	k	k_2	α	IF
1[b]	4.78	7.12	1.44	1.49	4.35	6.56	1.44	1.51	4.15	5.74	1.35	1.38
2[b]	5.02	6.20	1.20	1.24	4.63	5.64	1.16	1.22	4.42	5.15	1.15	1.17
3[b]	5.55	6.51	1.14	1.17	5.05	6.00	1.13	1.19	4.83	5.53	1.13	1.14
OTA	5.18	5.66	–	1.09	4.78	5.28	–	1.10	4.61	4.92	–	1.07

[a] For the chromatographic conditions see Fig. 4.
[b] Analytes **1**–**3** were employed as racemic mixtures.
[c] Enantioselectivity value ($\alpha = k_2/k_1$).
[d] Imprinting factor ($IF = k_{MIP}/k_{NIP}$).

to the other polymers. This result indicates that in the actual case the stereochemical features of the chiral template and functional monomer do not exert any significant influence on the binding properties. Obviously, the difference in the free energies of diastereomeric complexes is not very pronounced and therefore may be cancelled in the competing environment of the polymerization mixture. Alternatively, the induced stereoselective properties of the binding sites may be obscured by the dominating background of non-defined stereocenters generated from the methacrylate species in course of the polymerization reaction.

3.6. Amide vs. ester type functional monomer

In a further attempt to optimize the OTA selectivity of our MIPs, we synthesized a novel quinuclidine-type functional monomer by replacing the amide bond in Q-MAA by an ester functionality. It was anticipated that the incorporation of ester-type functional monomers (Q-MA) would allow a more precise control of the overall polarity of the resulting MIPs. Moreover, the complete deletion of the amide-NH groups in the MIPs should allow us to probe whether or not the amide functionality is involved in OTA binding.

For this purpose, ''amide-free'' **P8** was prepared employing a 1:1:3 molar ratio of OTA mimic **1** as the template, Q-MA as the functional entity and *t*-Bu-MA as the auxiliary monomer (see Table 1). Comparison of the chromatographic retention data obtained with **P8** with those of **P3** revealed a more pronounced retention and higher enantioselectivity for templates **1**, **2** and **3** with the ester-type polymer (see Table 4). For OTA, retention was also enhanced

Table 4
Comparison of molecular recognition properties of polymers **P3** and **P8** imprinted with mimic **1** comprising amide-type and ester-type functional monomers[a]

Analyte	Polymer							
	NIP	**P3**			NIP	**P8**		
	k	k_2	α[c]	IF[d]	k	k_2	α	IF
1[b]	4.78	7.12	1.44	1.49	6.45	10.39	1.52	1.61
2[b]	5.02	6.20	1.20	1.24	7.01	8.94	1.22	1.27
3[b]	5.55	6.51	1.14	1.17	7.65	9.47	1.19	1.24
OTA	5.18	5.66	–	1.09	6.87	7.49	–	1.09

[a] For the chromatographic conditions see Fig. 4.
[b] Analytes **1**–**3** were employed as racemic mixtures.
[c] Enantioselectivity value ($\alpha = k_2/k_1$).
[d] Imprinting factor ($IF = k_{MIP}/k_{NIP}$).

with **P8**, but the relative retention was unchanged (1.09 on both polymers). This clearly indicates that recognition and binding of OTA does not depend on the presence of amide functionalities in the MIPs. Rather ion-pairing and hydrophobic interactions, in combination with a pronounced shape selectivity, do control selective binding of OTA to the developed polymers in polar/protic media.

3.7. Testing of cross-selectivity

To identify the non-covalent interaction forces governing selective substrate binding of polymer **P3**, the chromatographic retention behavior of **1** was compared with that of OTA and a set of structural analogues (**10**–**19** and OTB, structures are depicted in Fig. 5). The rationale behind this selection was to provide a systematic assembly of ''deletion structures'', i.e., analytes which differ from **1** only in a single structural or functional feature. Consequently, changes in the retention behavior induced by these unique structural modifications may reveal the relative importance of specific intramolecular interaction increments to overall molecular recognition.

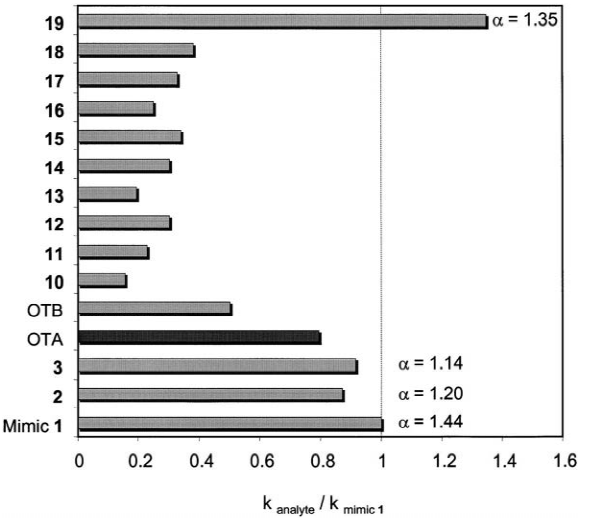

Fig. 6. Relative retention values of OTA, OTB, the racemic mimics **1**–**3** and structurally closely related test analytes **10**–**19**. In the case of **1**–**3** and **19** the (*S*)-enantiomer was more strongly retained. For the chromatographic conditions see Fig. 4.

The barchart given in Fig. 6 represents the changes in retention observed for the individual test analytes relative to OTA mimic **1** ($k_{\text{test compound}}$/

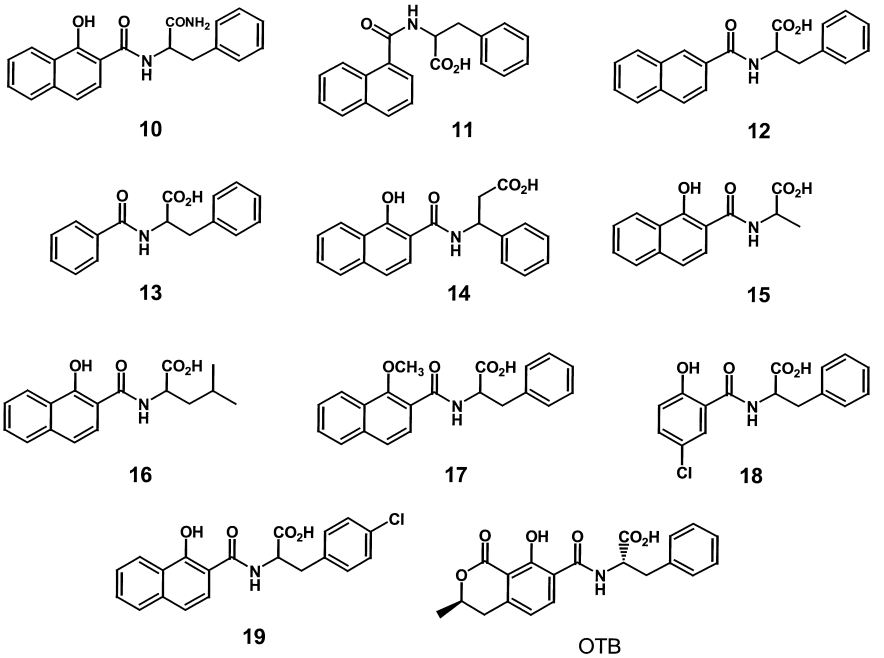

Fig. 5. Structures of the test analytes employed for evaluation of cross-selectivity of polymer **P3**.

$k_{\text{mimic 1}}$). Compounds **2**, **3** and OTA show relative retention values in the range of 0.8–1, reflecting the close structural resemblance to template **1**. This suggests that the binding cavities created by template **1** in the polymeric networks are well suited to accommodate these analytes. Unexpected strong binding is observed for compound **19**, which is structurally identical with the template but contains a 4-chloro substituent in the phenyl group of the amino acid side chain. Compound **10**, the amide derivative of **1**, is almost non-retained on **P3**. Obviously, the blocking of the carboxylic group leads to a substantial loss in affinity. This provides striking evidence that the overall binding is dominated by electrostatic interactions between the acidic analytes and the basic interaction centers, implemented by the quinuclidine-derived functional monomers.

Variations in the amino acid moiety in analytes **14**, **15** and **16** also result in a sharp decline in affinity. The introduction of aliphatic side chains (**15** and **16**) dramatically decreases the efficiency of molecular recognition, and binding is even impaired by replacing phenylalanine by the structurally closely related β-congener (**14**). From these observations, it is evident that the phenylalanine side chain does contribute to overall affinity, most probably acting as a spatially well-defined hydrophobic binding functionality. In a similar fashion, analyte retention is compromised by modifications of the naphthyl system. Reduction in the size of the aromatic system (**13** and **18**), deletion of the phenolic hydroxy group (**12**, **13** and **17**) and changes in the substitution pattern (**11**) all diminish retention relative to **1**. The rigid naphthyl moiety appears to be an important structural element, enhancing shape-complementarity with the binding sites and acting as platform for the pre-organization of the polar interaction sites. The loss in affinity and selectivity associated with the deletion and/or blocking of the phenolic hydroxy group suggests that this polar functionality may also support molecular recognition as an intermolecular or intramolecular hydrogen bond donor.

Although all analytes (except OTA and OTB as the respective enantiomers were not available) have been tested as racemic mixtures, enantioselectivity could be observed for the template **1** and analytes **2**, **3** and **19** only. Note that these compounds bear close structural resemblance to **1**, being different just due to the presence of an additional halide atom. In similar fashion, polymer **P3** is capable of distinguishing between OTA and OTB, the latter lacking a single chlorine, but being otherwise identical structures. These observations underline the high level of substrate selective binding achievable with **P3**. Thus, the combined use of carefully designed template mimics and functional monomers allows the generation of MIPs with highly substrate selective binding cavities in competing polar/protic media.

3.8. Influence of solvents on MIP affinity and selectivity

To achieve maximum clean-up and pre-concentration effects with MIP-based SPE materials, the impact of eluents and modifiers on selectivity and binding affinity has to be established carefully. Efficient removal of interfering matrix components and high recoveries require well-optimized adsorption and washing protocols, involving the consecutive use of different solvent systems. To provide basic knowledge about solvent effects on substrate selectivity and/or affinity of our ion-pairing type MIPs, the retention behavior of **1**, **2**, **3** and OTA was studied with polymer **P3**.

To assess the influence of the acidic modifier, the test compounds were chromatographed on **P3** with mobile phases comprising of methanol or chloroform and 1, 3 and 5% acetic acid, respectively. The corresponding retention, imprint and enantioselectivity values are summarized in Tables 5 and 6. Decreasing the content of acetic acid from 5 to 1% in methanol did enhance retention, enantioselectivity as well as imprint factors for template molecule **1** and also for the structurally closely related analytes **2** and **3**. In the case of OTA, also a substantial gain in retention was achieved by reducing the concentration of acidic modifier in the mobile phase, but the improvement in terms of selectivity, as indicated by the corresponding imprint factors, was less prominent. This reflects the still significant structural differences between OTA and the mimic molecules.

As is evident from Table 6, similar trends for **1**, **2** and **3** are observed when chloroform is used instead of the protic methanol as the mobile phase component. Again, a lower concentration of acidic modifier enhances affinity and selectivity for these

Table 5
Influence of the concentration of acidic modifier on the molecular recognition characteristics of polymer **P3** in methanol as the mobile phase[a]

Analyte	5% Acetic acid				3% Acetic acid				1% Acetic acid			
	NIP	MIP[c]			NIP	MIP[c]			NIP	MIP[c]		
	k	k_2	α[d]	IF[e]	k	k_2	α	IF	k	k_2	α	IF
1[b]	4.78	7.12	1.44	1.49	7.42	11.86	1.51	1.60	18.83	32.40	1.59	1.72
2[b]	5.02	6.20	1.20	1.24	7.84	10.27	1.25	1.31	20.61	28.87	1.29	1.40
3[b]	5.55	6.51	1.14	1.17	8.69	10.63	1.18	1.22	22.92	30.41	1.22	1.33
OTA	5.18	5.66	–	1.09	8.96	10.18	–	1.14	28.78	36.73	–	1.28

[a] For other chromatographic conditions see Fig. 4.
[b] Analytes **1**–**3** were employed as racemic mixtures.
[c] Mimic **1** as template.
[d] Enantioselectivity value ($\alpha = k_2/k_1$).
[e] Imprinting factor ($IF = k_{MIP}/k_{NIP}$).

compounds. OTA, however, shows a surprisingly different behavior. Compared to the mimics **1**–**3**, the gain in retention for OTA is much less pronounced and the imprint factor does not improve significantly with decreasing acetic acid concentrations. This behavior may be rationalized on basis of the so-called porogen effect. It has been demonstrated for MIPs that re-binding of the templates is frequently most efficient from the solvents which were used as porogens during the polymerization processes [15,35–37]. This memory effect may be associated with favorable solvation phenomena, which allow us to regenerate the ''active'' form of the binding cavities in the MIPs. In the actual case, chloroform seems to solvate the binding cavities in a way that facilitates the re-binding of the template and closely related compounds quite well, but rejects molecules with more pronounced structural differences. As a general trend, however, lower concentrations of acidic modifier led to a strengthening of the dominating ion-pairing at the binding centers of the MIP. Moreover, the decrease in overall polarity of the mobile phase may also facilitate the favorable participation of weaker interaction forces, e.g., hydrogen bonding and hydrophobic increments, in the molecular recognition event.

In further chromatographic experiments, the molecular recognition properties of **P3** for mimics **1–3** and OTA in other solvents frequently employed in SPE protocols were investigated. The corresponding data obtained with mobile phases comprising of acetonitrile, chloroform and *tert.*-butyl methyl ether,

Table 6
Influence of the concentration of the acidic modifier on the molecular recognition characteristics of polymer **P3** in chloroform as the mobile phase[a]

Analyte	5% Acetic acid				3% Acetic acid				1% Acetic acid			
	NIP	MIP[c]			NIP	MIP[c]			NIP	MIP[c]		
	k	k_2	α[d]	IF[e]	k	k_2	α	IF	k	k_2	α	IF
1[b]	2.05	3.64	1.29	1.76	3.79	7.09	1.36	1.87	13.60	29.56	1.50	2.17
2[b]	2.94	4.18	1.00	1.42	5.69	8.90	1.14	1.56	20.96	35.98	1.22	1.72
3[b]	2.96	4.23	1.00	1.43	5.71	8.95	1.13	1.57	21.13	34.69	1.17	1.64
OTA	0.32	0.45	–	1.41	0.69	0.98	–	1.42	2.77	4.02	–	1.45

[a] For other chromatographic conditions see Fig. 4.
[b] Analytes **1**–**3** were employed as racemic mixtures.
[c] Mimic **1** as template.
[d] Enantioselectivity value ($\alpha = k_2/k_1$).
[e] Imprinting factor ($IF = k_{MIP}/k_{NIP}$).

Table 7
Influence of different solvents on the recognition properties of polymer **P3**[a]

Analyte	Methanol–acetic acid				Acetonitrile–acetic acid				Chloroform–acetic acid				*t*-Butyl methyl ether–acetic acid			
	NIP	MIP[c]			NIP	MIP[c]			NIP	MIP[c]			NIP	MIP[c]		
	k	k_2	α[d]	IF[e]	k	k_2	α	IF	k	k_2	α	IF	k	k_2	α	IF
1[b]	4.78	7.12	1.44	1.49	5.58	7.87	1.25	1.41	2.05	3.64	1.29	1.76	5.93	11.41	1.52	1.92
2[b]	5.02	6.20	1.20	1.24	7.07	8.68	1.08	1.23	2.94	4.18	1.00	1.42	5.09	7.67	1.20	1.51
3[b]	5.55	6.51	1.14	1.17	7.38	8.93	1.08	1.21	2.96	4.23	1.00	1.43	5.37	7.91	1.17	1.47
OTA	5.18	5.66	–	1.09	2.80	3.34	–	1.19	0.32	0.45	–	1.41	8.67	10.43	–	1.20

[a] For other chromatographic conditions see Fig. 4.
[b] Analytes **1**–**3** were employed as racemic mixtures.
[c] Mimic **1** as template.
[d] Enantioselectivity value ($\alpha = k_2/k_1$).
[e] Imprinting factor ($IF = k_{MIP}/k_{NIP}$).

respectively, and 5% acetic acidic as the modifier, are listed in Table 7. Retention for the analytes was most pronounced in *tert.*-butyl methyl ether and OTA was more strongly retained than any of the mycotoxin mimics in this solvent. In contrast, this picture was reversed in chloroform, the solvent used as the porogen in MIP production. Here, the lowest values for the retention factors were observed, with OTA much less effectively retained than the mimics. In acetonitrile, **P3** retained the mimics **1**–**3** quite effectively, while OTA showed significantly less affinity. With methanol as the mobile phase, retention factors for the mimics and OTA were in a comparable range. In terms of enantioselectivity, the relatively apolar *tert.*-butyl methyl ether is superior to methanol, followed by acetonitrile and chloroform. OTA selectivity, as expressed by the imprinting factors, is most favorable with chloroform, in the same range for *tert.*-butyl methyl ether and acetonitrile and relatively poor in methanol.

Based on this set of information, efficient SPE protocols based on MIP **P3** might be developed. Strong retention observed for OTA in *tert.*-butyl methyl ether recommends this solvent as a trapping medium of the mycotoxin from matrix-rich extracts. Selective removal of neutral matrix components may be achieved by washing steps, employing pure solvents. The strong electrostatic binding of OTA to **P3** may also allow us to use eluents containing small amounts of acidic modifiers. To maximize pre-concentration and clean-up effects, OTA may be eluted from **P3** employing solvents like chloroform containing acidic modifiers. Alternatively, if the presence of organic solvents interferes with the analytical method used for quantification, e.g., reversed-phase chromatography, OTA can be eluted conveniently with acetonitrile without sacrificing the advantage of efficient pre-concentration.

*3.9. Determination of binding capacity of **P3***

Ideally, efficient MIP-based SPE materials should display, apart from high affinity and selectivity, appreciable binding capacities for the analyte of interest. If these requirements are fulfilled, SPE can be performed with rather small amounts of polymer, allowing the reduction or even suppression of non-selective adsorption effects.

To determine the binding capacity of **P3** for template molecule **1**, frontal analysis experiments were carried out [32]. Analysis of the chromatographic data gave a total binding capacity of 195 μmol template **1**/g dry polymer. The relatively steep shape of the frontal analysis curve indicates a favorable characteristic of **P3** for SPE application. Thus, even at a sample loading of 170 μmol/g dry MIP only 5% breakthrough of **1** was observed. The bromine and chlorine content of dry **P4** and **P5** (established by elemental analysis) after template extraction suggests successful removal of 95% of the imprint molecules **2** and **3**, initially incorporated into the polymeric matrices. Assuming a similar extraction yield for **P3**, the binding capacity determined above corresponds to 90% template re-binding. This high value is generally not found with conventional non-covalently imprinted polymers due to irrevers-

ible binding site collapse on template elution [17,32,35,38]. This confirms that **P3** rather behaves as a ''non-covalent stoichiometric'' imprinted polymer, which displays superior characteristics in terms of binding site homogeneity and re-binding capacity [39]. Clearly, these advantageous features of **P3** may further facilitate the development of highly selective SPE protocols.

4. Conclusions

Novel MIPs capable of recognizing OTA have been prepared using rationally designed analyte mimics as templates. A set of novel functional monomers was developed to address the individual structure elements of OTA. Strongly basic quinuclidine-type momomers were implemented to facilitate OTA binding in polar/protic media via ion-pairing interactions. Binding of the hydrophobic domains of OTA was promoted by sterically demanding and highly lipophilic auxiliary monomers. Polymers prepared with an 1:1:3 molar ratio of acidic OTA mimics, basic functional and hydrophobic auxiliary monomers showed superior recognition properties compared to materials generated with excess amounts of basic functional monomer. Under chromatographic conditions, the imprinted polymers display appreciable affinity and enantioselectivity for the OTA mimics used as templates as well as for OTA. The polymers show a pronounced substrate selectivity, suggesting the existence of binding cavities which discriminate between structurally closely related analytes based on electrostatic, hydrophobic and steric interaction increments. The OTA affinity of the polymers can be tuned by the nature of the solvent and/or the concentration of acidic modifier in the mobile phase. Increasing amounts of acetic acid weaken OTA binding to the polymers in all solvents, demonstrating the dominating role of electrostatic interactions. Affinity for OTA is most pronounced in *tert*.-butyl methyl ether, while binding is weak in chloroform. Retention of OTA can also be achieved in polar and/or protic environments such as acetonitrile and methanol. The favorable combination of high binding capacity, broad solvent compatibility and the OTA affinity make these polymers promising candidates for selective SPE applications. Currently, these materials are under evaluation in our laboratories as selective SPE adsorbents for real-world samples.

Acknowledgements

This project was supported by the Österreichische Nationalbank through grant No. 7528. We thank E. Gavioli, M.E. Martin Fernandez and G. Buttinger for assistance in the syntheses and M.P. Franco Puertolas and A. Leitner for the critical review of the manuscript. The authors are indebted to D. Lubda (Merck, Darmstadt, Germany) for providing the HPLC cartridges employed for the evaluation of the molecularly imprinted polymers.

References

[1] P. Krogh, in: P. Krogh (Ed.), Mycotoxins in Food, Academic Press, London, 1987, p. 97.
[2] P.M. Scott, in: J.D. Miller, H.L. Trenholm (Eds.), Mycotoxins in Grain—Compounds Other Than Aflatoxin, Eagan Press, St. Paul, 1997, p. 261.
[3] M. Weidenbörner, Encyclopedia of Food Mycotoxins, Springer, Heidelberg, 2001.
[4] B. Zimmerli, R. Dick, Food Addit. Contam. 13 (1996) 655.
[5] E.E. Creppy, J. Toxicol., Toxin Rev. 18 (1999) 277.
[6] H. Valenta, J. Chromatogr. A 815 (1998) 75, and references cited therein.
[7] P. Zöllner, A. Leitner, D. Lubda, K. Cabrera, W. Lindner, Chromatographia 52 (2000) 818.
[8] A. Leitner, P. Zöllner, A. Paolillo, J. Stroka, A. Papadopoulou-Bouraoui, S. Jaborek, E. Anklam, W. Lindner, Anal. Chim. Acta, in press.
[9] A. Biancardi, A. Riberzani, J. Liq. Chromatogr. Rel. Technol. 19 (1996) 2395.
[10] P.M. Scott, M.W. Trucksess, J. AOAC Int. 80 (1997) 941.
[11] A. Visconti, M. Pascale, G. Centonze, J. Chromatogr. A 864 (1999) 89.
[12] B. Zimmerli, R. Dick, J. Chromatogr. B 666 (1995) 85.
[13] P.K. Owens, L. Karlsson, E.S.M. Lutz, L.I. Andersson, Trends Anal. Chem. 18 (1999) 146.
[14] L.I. Andersson, J. Chromatogr. B 739 (2000) 163.
[15] D. Stevenson, Trends Anal. Chem. 18 (1999) 154.
[16] F. Lanza, B. Sellergren, Chromatographia 53 (2001) 599.
[17] G. Wulff, Angew. Chem. Int. Ed. 34 (1995) 1812.
[18] A.G. Mayes, K. Mosbach, Trends Anal. Chem. 16 (1997) 321.
[19] B. Sellergren, Trends Anal. Chem. 16 (1997) 310.
[20] T. Takeuchi, J. Haginaka, J. Chromatogr. B 728 (1999) 1.

[21] L.I. Andersson, A. Paprica, T. Arvidsson, Chromatographia 46 (1997) 57.
[22] L.I. Andersson, Analyst 125 (2000) 1515.
[23] J. Matsui, K. Fujiwara, S. Ugata, T. Takeuchi, J. Chromatogr. A 889 (2000) 25.
[24] J. Matsui, K. Fujiwara, T. Takeuchi, Anal. Chem. 72 (2000) 1810.
[25] M. Quaglia, K. Chenon, A.J. Hall, E.D. Lorenzi, B. Sellergren, J. Am. Chem. Soc. 123 (2001) 2146.
[26] R.F. Venn, R.J. Goody, Chromatographia 50 (1999) 407.
[27] J. Haginaka, H. Sanbe, Anal. Chem. 72 (2000) 5206.
[28] J. Heyboer, A.J. Staverman, Rec. Trav. Chim. 69 (1950) 787.
[29] G.A. Olah, S.C. Narang, B.G. Gupta, R. Malhorta, J. Org. Chem. 44 (1979) 1247.
[30] H. Weil, Chem. Ber. 44 (1911) 3058.
[31] W. Oberleitner, Thesis, University of Vienna, Vienna, 2000.
[32] M. Kempe, K. Mosbach, Anal. Lett. 24 (1991) 1137.
[33] B. Sellergren, M. Lepistoe, K. Mosbach, J. Am. Chem. Soc. 110 (1988) 5853.
[34] C. Dauwe, B. Sellergren, J. Chromatogr. A 753 (1996) 191.
[35] B. Sellergren, K.J. Shea, J. Chromatogr. 635 (1993) 31.
[36] B.A. Rashid, R.J. Briggs, J.N. Hay, D. Stevenson, Anal. Commun. 34 (1997) 303.
[37] I. Ferrer, F. Lanza, A. Tolokan, V. Horvath, B. Sellergren, G. Horvai, D. Barceló, Anal. Chem. 72 (2000) 3934.
[38] B. Sellergren, Macromol. Chem. 190 (1989) 2703.
[39] G. Wulff, R. Schoenfeld, Adv. Mater. 10 (1998) 957.